ChemComm

COMMUNICATION

View Article Online
View Journal | View Issue

Cite this: *Chem. Commun.*, 2018, 54, 10199

Received 9th July 2018,
Accepted 13th August 2018

DOI: 10.1039/c8cc05505j

rsc.li/chemcomm

Z-Schematic and visible-light-driven CO_2 reduction using H_2O as an electron donor by a particulate mixture of a Ru-complex/$(CuGa)_{1-x}Zn_{2x}S_2$ hybrid catalyst, $BiVO_4$ and an electron mediator†

Tomiko M. Suzuki,*[a] Shunya Yoshino,[b] Tomoaki Takayama,[b] Akihide Iwase,[b] Akihiko Kudo*[b] and Takeshi Morikawa[a]

Visible-light-driven Z-schematic CO_2 reduction using H_2O as an electron donor was achieved using a simple mixture of a metal-sulfide/molecular hybrid photocatalyst for CO_2 reduction, a water oxidation photocatalyst and a redox-shuttle electron mediator. This is the first demonstration of a highly selective particulate CO_2 reduction system accompanying O_2 generation utilizing a semiconductor/molecular hybrid photocatalyst.

Photocatalytic CO_2 reduction into useful energy-rich chemicals using water as an electron donor with a particulate system has attracted attention for sustainable and scalable artificial photosynthesis to mitigate global warming and generate useful fuels.[1–5] Particulate systems are recognized as cost-effective and could be the ultimate tool for CO_2 fixation and solar fuel generation.[6,7] A photocatalytic Z-scheme (or two-step photoexcitation) system that connects photocatalysts for CO_2 reduction with H_2O oxidation is considered to be a promising approach; however, few particulate Z-scheme systems for CO_2 reduction using water as an electron donor have been reported. Visible-light-driven conversion of CO_2 into CO over a combined system of CoO_x-loaded $BiVO_4$ and metal sulfides with a reduced graphene oxide electron mediator has yet to reach 1% CO selectivity. This is due to competitive H_2 generation and low CO_2 selectivity at metal sulfide surfaces.[8,9]

A hybrid catalyst of a semiconductor[10–12] linked with a metal-complex catalyst[13–15] is promising for visible-light-driven selective CO_2 reduction with regard to high selectivity, depending on the selective coordination of CO_2 molecules to the metal centers of the complexes.[13,16–22] It is essential that photoexcited electrons in the conduction band (CB) of the semiconductor transfer to the metal-complex catalyst within the picosecond region, which leads to two-electron reduction of CO_2 at the complex.[23] We previously demonstrated solar formate generation from CO_2 and H_2O using a photocathode of a Ru-complex catalyst linked with Zn-doped InP or N,Zn-codoped Fe_2O_3 combined with TiO_2 or $SrTiO_{3-x}$ photoanodes,[24–26] and confirmed the potential of the system with a solar-to-chemical conversion efficiency of 4.6% over a monolithic Ru-complex-polymer/Si–Ge/IrO_x electrode.[27] Ishitani and colleagues reported photoelectrochemical CO_2 reduction to CO *via* H_2O oxidation using a photocathode composed of a Ru(II)–Re(I) supramolecular metal complex immobilized on a NiO or $CuGaO_2$ semiconductor.[28,29] In contrast, a particulate system for Z-schematic CO_2 reduction using a metal complex combined with a H_2O oxidation reaction has not yet been demonstrated. Efficient electron transfer from the H_2O oxidation site to the CO_2 reduction site without degradation of the catalytic activity for both reactions should be implemented.

To realize Z-schematic CO_2 reduction with a particulate system, we focused our attention on metal sulfides as the CO_2 reduction semiconductor because they generally possess long photoexcited carrier lifetimes and narrow band gaps (BGs) originating from the S 3p state, which allows absorption of a substantial amount of visible light. Reisner *et al.* reported photocatalytic conversion of CO_2 into CO in water with >90% selectivity over a Ni–cyclam catalyst anchored with CdS.[19] We reported CO_2 photoconversion into HCOOH over ZnS:Ni and $(AgIn)_{0.22}Zn_{1.56}S_2$ linked with a Ru–bipyridine catalyst [Ru(4,4′-diphosphonate-2,2′-bipyridine)$(CO)_2Cl_2$] ([Ru(dpbpy)]).[30] These Cd- and Zn-based sulfides are considered to be beneficial when combined with molecular catalysts because of their negative CB minimum (E_{CBM}) positions originating from Cd 5s5p and Zn 4s4p orbitals, respectively, which facilitate fast electron transfer from the CB in a photoexcited state to a metal-complex catalyst due to the greater energy difference (ΔG) between the E_{CBM} and CO_2 reduction potential of the metal-complex, which promotes the CO_2 reduction reaction. However, these systems conducted half reactions that required triethanolamine as a strong

[a] *Toyota Central R&D Labs., Inc., 41-1 Yokomichi, Nagakute, Aichi 480-1192, Japan. E-mail: tomiko@mosk.tytlabs.co.jp*
[b] *Department of Applied Chemistry, Tokyo University of Science, 1-3 Kagurazaka, Shinjuku-ku, Tokyo 162-8601, Japan. E-mail: a-kudo@rs.kagu.tus.ac.jp*

† Electronic supplementary information (ESI) available: Experimental details, XRD patterns, UV-vis diffuse reflectance spectra, Z-schematic CO_2 reduction using a hybrid photocatalyst, $BiVO_4$ and a Co-complex, GC-MS chromatograms, IC-TOFMS chromatograms, and XPS spectra. See DOI: 10.1039/c8cc05505j

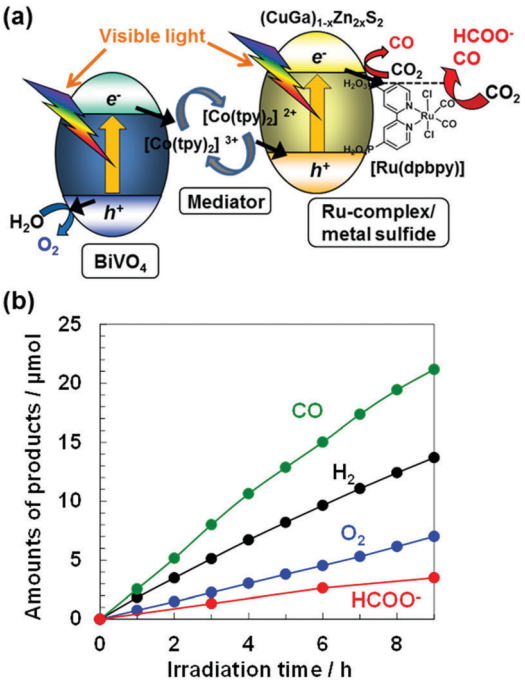

Fig. 1 (a) Visible-light-driven Z-schematic system for CO_2 reduction consisting of particulate [Ru(dpbpy)] modified $(CuGa)_{1-x}Zn_{2x}S_2$ hybrid photocatalysts, a $BiVO_4$ photocatalyst, and a $[Co(tpy)_2]^{3+/2+}$ redox shuttle electron mediator. (b) Z-schematic CO_2 reduction in an aqueous solution with a CO_2 flow system. Conditions: [Ru(dpbpy)]/$(CuGa)_{0.3}Zn_{1.4}S_2$ (0.4 g) and $BiVO_4$ (0.2 g); 0.02 mM $[Co(tpy)_2]^{2+}$ containing 0.1 M $NaHCO_3$ aqueous solution (150 mL) and visible-light ($\lambda > 420$ nm).

sacrificial electron donor. Here, we demonstrate the first particulate-based visible-light-driven Z-scheme system that harmonizes both reactions of CO_2 reduction and H_2O oxidation over a hybrid photocatalyst of a semiconductor/molecular-catalyst.

Fig. 1(a) shows an illustration of the Z-schematic system for photoconversion of CO_2 to CO and $HCOO^-$ over [Ru(dpbpy)]-modified $(CuGa)_{1-x}Zn_{2x}S_2$ as a CO_2 reduction hybrid photocatalyst, $[Co(tpy)_2]^{3+/2+}$ (tpy: 2,2′:6,2″-terpyridine) as an electron mediator, and $BiVO_4$ as a water oxidation photocatalyst. Fig. 1(b) shows that the simple mixture in an aqueous solution produced CO and $HCOO^-$ at almost linear rates together with O_2 generation under visible light irradiation after hours of pre-irradiation in a CO_2 flow reactor,[8,9] *i.e.*, the Z-scheme reaction. Although $BiVO_4$ can photogenerate O_2, E_{CBM} for $BiVO_4$ is located at an unfavorably deep position for the reduction reaction of CO_2 and protons.[8,31] Thus, the CO_2 reduction reaction could occur at the [Ru(dpbpy)]/$(CuGa)_{0.3}Zn_{1.4}S_2$ photocatalyst, which suggests a Z-scheme mechanism with H_2O as an electron donor, which is discussed later. Although H_2 evolution by proton reduction also proceeded, the CO_2 reduction selectivity to total reductive products (CO, $HCOO^-$, H_2) for 9 h reached 64 mol%, significantly higher than the *ca.* 1% of previous non-molecular particulate Z-scheme systems.[8,9] The modification of [Ru(dpbpy)] led to the production of $HCOO^-$ and the turnover number (TON) of $HCOO^-$ evolution was calculated to be 17, assuming that all [Ru(dpbpy)] remained on $(CuGa)_{1-x}Zn_{2x}S_2$ during the photocatalytic reaction.

The key to designing the visible-light-driven Z-schematic system is the hybrid photocatalyst for CO_2 reduction. Thus, a sufficient energy difference ΔG to facilitate fast electron transfer from the semiconductor to the Ru-complex catalyst plays a decisive role.[16,23] Electron transfer from the water oxidation photocatalyst to the CO_2 reduction photocatalyst is also indispensable. First, the optimal combination of Ru-complex and semiconductor was investigated. A solid solution of $CuGaS_2$ and ZnS ($(CuGa)_{1-x}Zn_{2x}S_2$)[32] was selected as the semiconductor for the hybrid photocatalyst because their BG and band position, particularly E_{CBM}, are dominated by Zn 4s4p + Ga 4s4p and are tunable by changing x. This could be beneficial to control the electron transfer rate from the CB to the molecular catalysts. XRD measurements of $(CuGa)_{1-x}Zn_{2x}S_2$ synthesized by a solid-state reaction[32] revealed that a single chalcopyrite phase ($x \leq 0.2$) or zincblende structure ($x \geq 0.5$) was obtained (Fig. S1 and Table S1, ESI†). The BG of $CuGaS_2$ and $(CuGa)_{1-x}Zn_{2x}S_2$ ($x < 1.0$) was within the range of 2.24–2.54 eV, which enables absorption of visible light (Fig. S2 and Table S1, ESI†). Hybrid catalysts of 0.03–0.08 wt% [Ru(dpbpy)] with the phosphonate ligand (CO_2 reduction potential of *ca.* −1.0 V *vs.* NHE)[30] linked with $(CuGa)_{1-x}Zn_{2x}S_2$ were prepared using an adsorption method[30] (Table S2, ESI†).

Typical Z-schematic CO_2 reduction was performed by using [Ru(dpbpy)]/$(CuGa)_{1-x}Zn_{2x}S_2$ and $BiVO_4$ in a test tube filled with $[Co(tpy)_2]^{2+}$ containing aqueous $NaHCO_3$ solution saturated with CO_2 under visible light irradiation for 16 h. This method is useful to measure the tendency of the sample-dependent product for multiple runs.[33] Fig. 2(a) shows that the CO_2 reduction activity was significantly dependent on the composition of $(CuGa)_{1-x}Zn_{2x}S_2$. For bare $(CuGa)_{1-x}Zn_{2x}S_2$, the amount of CO produced increased with x within the range of $0.0 \leq x \leq 0.5$, which could be explained by the more negative E_{CBM} and narrower BG (Fig. 2(b) and Fig. S2, ESI†), which led to a more efficient electron transfer toward a higher CO_2 reduction rate. Further increase in x ($x \geq 0.7$) decreased CO evolution due to a reduced amount of absorbed photons with a wider BG (≥2.36 eV). H_2 evolution induced by the competitive proton reduction increased with x within the range of $0.5 \leq x \leq 0.7$. Replacement of the bare $(CuGa)_{1-x}Zn_{2x}S_2$ with the [Ru(dpbpy)]/$(CuGa)_{1-x}Zn_{2x}S_2$ hybrid photocatalyst not only enhanced the CO formation rate but also induced formate production; [Ru(dpbpy)] is known as a catalyst for the production of formate and CO.[30,34] [Ru(dpbpy)]/$(CuGa)_{1-x}Zn_{2x}S_2$ at $x = 0.7$ showed the highest CO_2 reduction activity for CO and $HCOO^-$ production, with TONs (based on product generated by the [Ru(dpbpy)] catalyst) of 214 and 70 after 16 h of reaction, respectively. In the Z-schematic water splitting system composed of metallic Ru-loaded $(CuGa)_{1-x}Zn_{2x}S_2$ for H_2 generation, CoO_x-loaded $BiVO_4$ for water oxidation and $[Co(tpy)_2]^{2+/3+}$ for electron mediation, the highest water splitting rate was reported at $x = 0.2$.[32] In contrast, [Ru(dpbpy)]/$(CuGa)_{0.8}Zn_{0.4}S_2$ ($x = 0.2$) showed a negligibly small CO_2 reduction activity. These results suggest that more negative E_{CBM} (with greater x) improves the electron transfer rate for CO_2 reduction at [Ru(dpbpy)].[16,17,23,30] The CO_2 reduction activity of the hybrid catalyst is in a trade-off relationship between

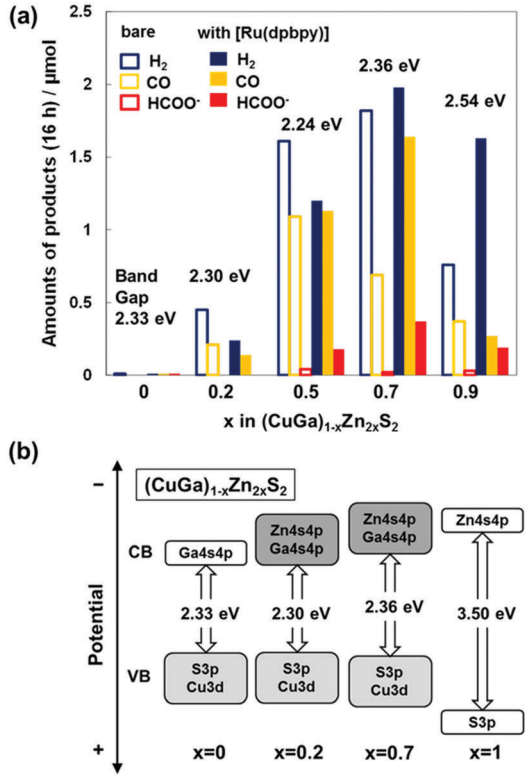

Fig. 2 (a) Z-Schematic CO_2 reduction using the $(CuGa)_{1-x}Zn_{2x}S_2$ or ([Ru(dpbpy)]/$(CuGa)_{1-x}Zn_{2x}S_2$)–($[Co(tpy)_2]^{3+/2+}$)–($BiVO_4$) systems under visible-light irradiation using the test tube method. Conditions: 8 mg of each photocatalyst; 0.02 mM $[Co(tpy)_2]^{2+}$ containing 0.1 M $NaHCO_3$ aqueous solution (4 mL); visible-light ($390 < \lambda \leq 750$ nm) for 16 h. (b) Estimated band structures of $(CuGa)_{1-x}Zn_{2x}S_2$.

the negative E_{CBM} to facilitate electron transfer to the complex catalyst and the BG to determine the number of photons absorbed; therefore, overall matching in the electron transfer process was successful in the present Z-schematic ([Ru(dpbpy)]/$(CuGa)_{1-x}Zn_{2x}S_2$)–($[Co(tpy)_2]^{3+/2+}$)–($BiVO_4$) system.

Experimental data used to determine the effective components for the Z-schematic CO_2 reduction are summarized in Table 1. A mixture of $BiVO_4$ and $[Co(tpy)_2]^{2+}$ produced neither H_2, nor CO, nor $HCOO^-$ due to the unfavorably deep E_{CBM} position (entry 1). The addition of $(CuGa)_{0.3}Zn_{1.4}S_2$ produced H_2 and CO (entry 2), and [Ru(dpbpy)] modification of $(CuGa)_{0.3}Zn_{1.4}S_2$ induced $HCOO^-$ formation and further improved CO production by the effect of [Ru(dpbpy)] (entry 3, Fig. S3, ESI†). The absence of $[Co(tpy)_2]^{2+}$ largely decreased CO and $HCOO^-$ generation (entry 4), and removal of $BiVO_4$ resulted in the termination of both CO and $HCOO^-$ formation (entry 5, Fig. S4, ESI†). These results indicate that $BiVO_4$ is necessary for high CO_2 reduction activity, and the presence of $[Co(tpy)_2]^{2+}$ is essential for a high CO and $HCOO^-$ formation rate. The absence of $NaHCO_3$ decreased the formation of both CO and $HCOO^-$ (entry 6), and the formation of CO and $HCOO^-$ was negligible in the absence of $[Co(tpy)_2]^{2+}$ (entry 7). Among the aqueous electrolyte and Co-complexes, $NaHCO_3$ and $[Co(tpy)_2]^{2+}$ were evaluated to be the best for the CO_2 reduction selectivity and production rate, respectively (Tables S3 and S4, ESI†). It was also confirmed that no reaction occurred without irradiation (entry 8), and that the formation of CO and $HCOO^-$ was negligibly small when Ar was bubbled in the solution (entry 9).

$[Co(tpy)_2]^{2+}$ was reported to act as a $[Co(tpy)_2]^{3+/2+}$ redox shuttle electron mediator connecting two semiconductors for H_2 and O_2 generation in Z-scheme water splitting.[32] As inferred from the mechanism of the IO_3^-/I^- shuttle redox mediator system,[35,36] it is speculated that $[Co(tpy)_2]^{3+}$ may favorably adsorb onto $BiVO_4$, while $[Co(tpy)_2]^{2+}$ adsorbs onto $(CuGa)_{0.3}Zn_{1.4}S_2$, mediating electrons between them as a redox shuttle. $[Co(tpy)_2]^{2+}$ was reported to be an electrocatalyst for the reduction of CO_2 to CO in dimethylformamide/H_2O (90/10 v/v) when one terpyridine ligand was eliminated.[37,38] However, the intrinsic potential for the reaction is too negative (−2.0 V *vs.* Fc/Fc^+) compared to the E_{CBM} of $(CuGa)_{0.3}Zn_{1.4}S_2$; therefore, $[Co(tpy)_2]^{2+}$ is not a catalyst in the present case. $[Co(tpy)_2]^{2+}$ did not catalyze CO_2 reduction in an aqueous solution when electrically biased in the E_{CBM} region under visible light irradiation.

Isotope tracer analyses using $^{13}CO_2$ confirmed that the carbon source of evolved CO and $HCOO^-$ was dissolved CO_2 (Fig. S5 and S6, ESI†). O_2 was also confirmed to originate from water using $H_2{}^{18}O$ (Fig. S7, ESI†), in which the total amount of $^{18}O_2$ and $^{16}O^{18}O$ was more than 85% of the total dioxygen detected.

Table 1 Z-Schematic CO_2 reduction activity of the ([Ru(dpbpy)]/$(CuGa)_{0.3}Zn_{1.4}S_2$)–($[Co(tpy)_2]^{3+/2+}$)–($BiVO_4$) system under visible-light irradiation for 16 h[a]

	CO_2 reduction photocatalyst		Mediator	O_2 evolution photocatalyst	Salt			Amount of products (μmol)		
Entry	$(CuGa)_{0.3}Zn_{1.4}S_2$	[Ru(dpbpy)]	$[Co(tpy)_2]^{2+}$	$BiVO_4$	$NaHCO_3$	Gas	$h\nu$	H_2	CO	$HCOO^-$
1			✓	✓	✓	CO_2	✓	0.00	0.00	0.00
2	✓		✓	✓	✓	CO_2	✓	1.82	0.69	0.02
3	✓	✓	✓	✓	✓	CO_2	✓	1.98	1.64	0.37
4	✓	✓		✓	✓	CO_2	✓	1.53	0.10	0.10
5	✓	✓	✓		✓	CO_2	✓	1.06	0.79	0.28
6	✓	✓	✓	✓		CO_2	✓	3.59	0.56	0.18
7	✓	✓		✓		CO_2	✓	2.42	0.01	0.02
8	✓	✓	✓	✓	✓	CO_2		0.00	0.00	0.00
9	✓	✓	✓	✓	✓	Ar	✓	0.96	0.01	0.01

[a] Conditions: 8 mg of each photocatalyst; 0.02 mM $[Co(tpy)_2]^{2+}$ containing 0.1 M $NaHCO_3$ aqueous solution (4 mL); visible-light ($390 < \lambda \leq 750$ nm) for 16 h; Pyrex test tube.

These results explained that CO_2 was reduced to CO and $HCOO^-$ using electrons extracted from H_2O molecules. The TON for O_2 evolution with the Co-complex was calculated to be 9 (9 h), which suggests that the Co-complex acted as an electron mediator. A slight deviation from stoichiometric O_2 evolution (4-electron reaction) compared with half of the total of CO + $HCOO^-$ + H_2 (2-electron reactions) in Fig. 1(b) was similarly observed in all-inorganic Z-scheme systems for CO_2 reduction.[8,9] Self-photooxidation of $(CuGa)_{1-x}Zn_{2x}S_2$ could partially supply electrons for the CO_2 reduction reaction. Further investigations will clarify the overall electron/hole stoichiometry. X-ray photoelectron spectroscopy (XPS) measurements before and after the Z-scheme reaction (in Fig. 1(b)) revealed no change in the chemical state of Ru and sulfur ions (Fig. S8, ESI†). Half of the amount of [Ru(dpbpy)] was eliminated from the $(CuGa)_{1-x}Zn_{2x}S_2$ surface according to the change in the Ru/S and Ru/Zn ratios (Table S5, ESI†).

In conclusion, a visible-light-driven Z-schematic CO_2 reduction to CO and $HCOO^-$ in an aqueous particulate suspension system was achieved using a simple mixture of [Ru(dpbpy)]/$(CuGa)_{1-x}Zn_{2x}S_2$ hybrid, $[Co(tpy)_2]^{2+}$ and $BiVO_4$. Adjustment of band alignment is essential to the Z-schematic CO_2 reduction reaction accompanying O_2 generation. The very high CO_2 reduction selectivity beyond 60% against competing H_2 generation strongly suggests that the particulate Z-schematic system is feasible to construct selective and efficient photocatalysts for CO_2 fixation and solar fuel generation.

This work was partially supported by the JST ACT-C Grant Number JPMJCR12ZA, Japan (T. M. S. and T. M.). The authors thank Ms Ayako Oshima, Mr Kosuke Kitazumi, Ms Naoko Takahashi, Mr Satoru Kosaka, Mr Ikoma Narita and Ms Saori Narita for experimental assistance. The authors also thank Dr Shunsuke Sato, Dr Keita Sekizawa, and Dr Hiromitsu Tanaka for fruitful discussions.

Conflicts of interest

There are no conflicts to declare.

Notes and references

1 W. Kim, G. Yuan, B. A. McClure and H. Frei, *J. Am. Chem. Soc.*, 2014, **136**, 11034–11042.
2 A. M. Appel, J. E. Bercaw, A. B. Bocarsly, H. Dobbek, D. L. DuBois, M. Dupuis, J. G. Ferry, E. Fujita, R. Hille, P. J. Kenis, C. A. Kerfeld, R. H. Morris, C. H. Peden, A. R. Portis, S. W. Ragsdale, T. B. Rauchfuss, J. N. Reek, L. C. Seefeldt, R. K. Thauer and G. L. Waldrop, *Chem. Rev.*, 2013, **113**, 6621–6658.
3 J. L. White, M. F. Baruch, J. E. Pander III, Y. Hu, I. C. Fortmeyer, J. E. Park, T. Zhang, K. Liao, J. Gu, Y. Yan, T. W. Shaw, E. Abelev and A. B. Bocarsly, *Chem. Rev.*, 2015, **115**, 12888–12935.
4 H. Dau, E. Fujita and L. Sun, *ChemSusChem*, 2017, **10**, 4228–4235.
5 M. Wang, V. Artero, L. Hammarstrom, J. Martinez, J. Karlsson, D. Gust, P. Summers, C. Machan, P. Brueggeller, C. D. Windle, Y. Kageshima, R. Cogdell, K. R. Tolod, A. Kibler, D. H. Apaydin, E. Fujita, J. Ehrmaier, S. Shima, E. Gibson, F. Karadas, A. Harriman, H. Inoue, A. Kudo, T. Takayama, M. Wasielewski, F. Cassiola, M. Yagi, H. Ishida, F. Franco, S. O. Kang, D. Nocera, C. Li, F. Di Fonzo, H. Park, L. Sun, T. Setoyama, Y. S. Kang, O. Ishitani, J. R. Shen, H. J. Son and S. Masaoka, *Faraday Discuss.*, 2017, **198**, 353–395.
6 B. A. Pinaud, J. D. Benck, L. C. Seitz, A. J. Forman, Z. Chen, T. G. Deutsch, B. D. James, K. N. Baum, G. N. Baum, S. Ardo, H. Wang, E. Miller and T. F. Jaramillo, *Energy Environ. Sci.*, 2013, **6**, 1983–2002.
7 D. M. Fabian, S. Hu, N. Singh, F. A. Houle, T. Hisatomi, K. Domen, F. E. Osterloh and S. Ardo, *Energy Environ. Sci.*, 2015, **8**, 2825–2850.
8 A. Iwase, S. Yoshino, T. Takayama, Y. H. Ng, R. Amal and A. Kudo, *J. Am. Chem. Soc.*, 2016, **138**, 10260–10264.
9 T. Takayama, K. Sato, T. Fujimura, Y. Kojima, A. Iwase and A. Kudo, *Faraday Discuss.*, 2017, **198**, 397–407.
10 A. Kudo and Y. Miseki, *Chem. Soc. Rev.*, 2009, **38**, 253–278.
11 W. Kim, T. Seok and W. Choi, *Energy Environ. Sci.*, 2012, **5**, 6066–6070.
12 K. Li, B. Peng and T. Peng, *ACS Catal.*, 2016, **6**, 7485–7527.
13 G. Sahara and O. Ishitani, *Inorg. Chem.*, 2015, **54**, 5096–5104.
14 C. Costentin, M. Robert, J. M. Saveant and A. Tatin, *Proc. Natl. Acad. Sci. U. S. A.*, 2015, **112**, 6882–6886.
15 H. Takeda, C. Cometto, O. Ishitani and M. Robert, *ACS Catal.*, 2017, **7**, 70–88.
16 S. Sato, T. Morikawa, S. Saeki, T. Kajino and T. Motohiro, *Angew. Chem., Int. Ed.*, 2010, **49**, 5101–5105.
17 T. M. Suzuki, H. Tanaka, T. Morikawa, M. Iwaki, S. Sato, S. Saeki, M. Inoue, T. Kajino and T. Motohiro, *Chem. Commun.*, 2011, **47**, 8673–8675.
18 R. Kuriki, M. Yamamoto, K. Higuchi, Y. Yamamoto, M. Akatsuka, D. Lu, S. Yagi, T. Yoshida, O. Ishitani and K. Maeda, *Angew. Chem., Int. Ed.*, 2017, **56**, 4867–4871.
19 M. F. Kuehnel, K. L. Orchard, K. E. Dalle and E. Reisner, *J. Am. Chem. Soc.*, 2017, **139**, 7217–7223.
20 M. F. Kuehnel, C. D. Sahm, G. Neri, J. R. Lee, K. L. Orchard, A. J. Cowan and E. Reisner, *Chem. Sci.*, 2018, **9**, 2501–2509.
21 H. N. Tian, *ChemSusChem*, 2015, **8**, 3746–3759.
22 K. Sekizawa, K. Maeda, K. Domen, K. Koike and O. Ishitani, *J. Am. Chem. Soc.*, 2013, **135**, 4596–4599.
23 K. Yamanaka, S. Sato, M. Iwaki, T. Kajino and T. Morikawa, *J. Phys. Chem. C*, 2011, **115**, 18348–18353.
24 S. Sato, T. Arai, T. Morikawa, K. Uemura, T. M. Suzuki, H. Tanaka and T. Kajino, *J. Am. Chem. Soc.*, 2011, **133**, 15240–15243.
25 T. Arai, S. Sato, T. Kajino and T. Morikawa, *Energy Environ. Sci.*, 2013, 6.
26 K. Sekizawa, S. Sato, T. Arai and T. Morikawa, *ACS Catal.*, 2018, **8**, 1405–1416.
27 T. Arai, S. Sato and T. Morikawa, *Energy Environ. Sci.*, 2015, **8**, 1998–2002.
28 G. Sahara, H. Kumagai, K. Maeda, N. Kaeffer, V. Artero, M. Higashi, R. Abe and O. Ishitani, *J. Am. Chem. Soc.*, 2016, **138**, 14152–14158.
29 H. Kumagai, G. Sahara, K. Maeda, M. Higashi, R. Abe and O. Ishitani, *Chem. Sci.*, 2017, **8**, 4242–4249.
30 T. M. Suzuki, T. Takayama, S. Sato, A. Iwase, A. Kudo and T. Morikawa, *Appl. Catal., B*, 2018, **224**, 572–578.
31 Y. Xu, S. Wang, J. Yang, B. Han, R. Nie, J. Wang, J. Wang and H. Jing, *Nano Energy*, 2018, **51**, 442–450.
32 T. Kato, Y. Hakari, S. Ikeda, Q. Jia, A. Iwase and A. Kudo, *J. Phys. Chem. Lett.*, 2015, **6**, 1042–1047.
33 T. M. Suzuki, A. Iwase, H. Tanaka, S. Sato, A. Kudo and T. Morikawa, *J. Mater. Chem. A*, 2015, **3**, 13283–13290.
34 Y. Kuramochi, J. Itabashi, K. Fukaya, A. Enomoto, M. Yoshida and H. Ishida, *Chem. Sci.*, 2015, **6**, 3063–3074.
35 R. Abe, K. Sayama, K. Domen and H. Arakawa, *Chem. Phys. Lett.*, 2001, **344**, 339–344.
36 R. Abe, *Bull. Chem. Soc. Jpn.*, 2011, **84**, 1000–1030.
37 N. Elgrishi, M. B. Chambers, V. Artero and M. Fontecave, *Phys. Chem. Chem. Phys.*, 2014, **16**, 13635–13644.
38 N. Elgrishi, M. B. Chambers and M. Fontecave, *Chem. Sci.*, 2015, **6**, 2522–2531.

